Universality classes for phonon relaxation and thermal conduction in one-dimensional vibrational systems

Santhosh G.
Department of Physics, Indian Institute of Technology Madras, Chennai 600036, Tamil Nadu, India

Deepak Kumar
School of Physical Sciences, Jawaharlal Nehru University, New Delhi 110067, India

(Received 23 May 2011; published 14 October 2011)

We study phonon relaxation in chains of particles coupled through polynomial-type pair-interaction potentials and obeying quantum dynamics. We present detailed calculations for the sixth-order potential and find that the wave-vector-dependent relaxation rate follows a power-law behavior, $\Gamma(q) \sim q^{\delta}$, with $\delta = 5/3$, which is identical to that of the fourth-order potential. We argue through diagrammatic analysis that this is a generic feature of even-power potentials. Our earlier analysis has shown that $\delta = 3/2$ when the leading-order term in the nonlinear potential is odd, suggesting that there are two universality classes for the phonon relaxation rates dependent on a simple property of the potential. This implies that the thermal conductivity κ which diverges as a function of chain size N as $\kappa \propto N^{\alpha}$ also has two universal behaviors, in that $\alpha = 1 - 1/\delta$ as follows from a finite-size argument. We support these arguments by numerical calculations of conductivity for chains obeying classical dynamics for polynomial potentials of some even and odd powers.

DOI: 10.1103/PhysRevE.84.041119 PACS number(s): 05.70.Ln, 44.10.+i, 05.60.Gg, 66.25.+g

I. INTRODUCTION

In the larger context of understanding irreversibility of transport behavior on a microscopic basis, the study of thermal conduction in vibrational chains has received considerable attention [1,2]. In the last couple of decades, a number of numerical studies have established that the thermal conductivity shows a power-law divergence with the system size: $\kappa \sim N^{\alpha}$. The values of the exponent α for a variety of momentum-conserving systems, like vibrational chains with polynomial-type pair interactions with cubic or quartic powers [1,3], Toda lattice [4], particles with hard-core interactions [5], etc., strongly suggest the existence of a few universality classes for this behavior. The exponents seen cluster around two values, $\alpha = 1/3$ for vibrational chains with leading cubic nonlinearity and fluids and $\alpha = 2/5$ for chains with quartic potential. For quartic potential Mai *et al*. [6] have claimed that $\alpha = 1/3$ as well.

The concept of universality has found support in the analytical work as well. Narayan and Ramaswamy [7] made a renormalization group study of the hydrodynamic equations of heat transport to argue for a universal value of $\alpha = 1/3$ for all momentum-conserving systems in one dimension. The hydrodynamics arguments have been further refined by Lee-Dadswell *et al*. [8], who have argued for two universality classes depending on whether the specific heat ratio $\gamma = c_p/c_v$ is 1 ($\alpha = 1/2$) or greater than 1 ($\alpha = 1/3$). The classical vibrational chains have also been studied analytically by two methods: the mode-coupling method [9,10] and the kinetic theory method [11,12]. The mode-coupling treatment yields $\alpha = 1/3$ for cubic nonlinearity, and $\alpha = 1/2$ for the quartic nonlinearity in agreement with hydrodynamic arguments. The kinetic theory method has been applied for only the quartic potential and it yields $\alpha = 2/5$. A settlement of this issue is also hindered by the inherent complications of the problem: a precise definition of the size-dependent conductivity that can be used in calculations, the difficulty in analyzing the many-body problem with nonlinear interactions, and associated problems with approximations, numerical challenges, etc.

In view of the above, we have have recently treated this problem quantum mechanically [13–15]. To our mind this approach provides a different perspective on the problem, as well as allows us to make controlled and systematic approximations. In particular, we have calculated the thermal conductivity using the Kubo-Green formula for vibrational chains with various polynomial interactions. Since transport coefficients involve the lifetime of a quasiparticle state in a crucial way, the relaxation rate $\Gamma(q)$ (inverse liftime) of a phonon with wave vector q, in particular its dependence on q, is the key quantity in this calculation.

The phonon relaxation rate is calculated from the self-energy $\Sigma(q,\omega)$ through the equation $\Gamma(q) = -\mathrm{Im}\Sigma(q,\omega_q^R)$, where ω_q^R is the renormalized frequency of the phonon. $\Gamma(q)$ vanishes as the wave vector q goes to zero, $\Gamma(q) \sim q^{\delta}$, with the power $\delta > 1$ (otherwise the phonons cannot be regarded as well-defined quasiparticles). This makes the Kubo integral for thermal conductivity divergent in one dimension. But one can obtain the size dependence of the conductivity by introducing a time cutoff, proportional to the system size N, in the Kubo formula [1,7]. This gives the result $\alpha = 1 - 1/\delta$. If one follows this procedure, then the universality of thermal conduction is equivalent to the universality of δ, which is what we are studying in this paper.

The quantum version for the quartic potential was first analysed by us [13] following a crucial analysis of the collision integral of the modes [a precise definition of the term collision integral as used here is given later in Eq. (11)] by Pereverzev [11], whose classical treatment also led to a similar formulation. The key point here is that the noninteger power in the q dependence of the phonon relaxation rate $\Gamma(q)$ or self-energy arises due to the singular behavior of a second-order diagram as $q \to 0$. It turns out that all the higher-order diagrams, vertex corrections, etc., have an analytic dependence

on q and give rise to contributions of order q^2 to $\Gamma(q)$. These are therefore subdominant at small q, and this method yields $\delta = 5/3$ corresponding to $\alpha = 2/5$ for quartic nonlinearity. Another important point of the calculation is that the nonzero contribution comes from only the umklapp process, a feature that is not accounted for in classical calculations using mode-coupling analysis.

For the cubic potential a different set of arguments needs to be employed [14]. The second-order diagram does not contribute to the imaginary part of the self-energy as the wave-vector conservation and energy conservation cannot be satisfied together in a three-phonon process. Here we employed a self-consistent approach by allowing phonon lines a width, which is then calculated self-consistently through an integral equation [14]. This approach gives the phonon relaxation rate to be $\Gamma(q) \propto q^{3/2}$. This approach could be extended to higher-order potentials with odd nonlinearity, which give rise to numerous new processes but also include the second-order diagram with renormalized cubic interaction. It again transpires that except for this second-order diagram for the cubic potential, the other processes yield analytic contributions $O(q^2)$ to give leading contribution proportional to $q^{3/2}$. This enabled us to establish the existence of a universality class for thermal conduction and phonon relaxation corresponding to potentials containing any odd-power potential.

In this paper our aim is to analyze other even-power potentials to see if they follow a universal behavior. Our strategy is again to analyze the new processes that can occur with higher-order potentials and check if they can give rise to any singular dependences as $q \to 0$. Among the numerous new processes that arise with the higher-order potentials, one of them has the same structure as the one that becomes singular for the quartic potential. Apart from this one, we argue that the other processes give rise to analytic contributions of the form $\Gamma(q) \propto q^2$, though the explicit calculations are possible for fourth- and sixth-order potentials only. We also report numerical calculation of thermal conductivity for nonlinear potentials with even powers $n = 4$, 6, and 8. Within error margins of these calculations all these potentials show nearly identical values for α. We also confirm the previous numerical results for the cubic potential. For potentials with a leading odd-power nonlinearity and a lower bound, it suffices to consider the $n = 3$ case, as such a potential has a generic cubic order term. This makes the case for two universality classes for thermal conduction in vibrational chains, one corresponding to even potentials with $\alpha = 2/5$ and the other to potentials containing an odd power with $\alpha = 1/3$.

II. THE HAMILTONIAN

Consider a chain of N oscillators where only the nearest neighbors interact. The Hamiltonian of the system is given by

$$H = \sum_{l=1}^{N} \frac{p_l^2}{2m} + V(x_l - x_{l-1}), \tag{1}$$

where p_l and x_l are the momentum and position coordinates of the lth oscillator. We take the pair potential V to have the form

$$V(x) = \frac{1}{2} m\omega_0^2 x^2 + \frac{g_0}{n!} x^n, \tag{2}$$

n being an even integer. We use periodic boundary conditions and introduce phonon operators,

$$\begin{aligned} a_k &= \sqrt{\frac{m\omega_0\omega_k}{2\hbar}} \left(x_k + i \frac{p_k}{m\omega_0\omega_k} \right), \\ \omega(k) &= 2|\sin(k/2)|, \end{aligned} \tag{3}$$

where x_k and p_k are the usual Fourier transforms of x_l and p_l, respectively. The Hamiltonian, in units of $\hbar\omega_0$, becomes

$$\begin{aligned} H = \sum_k \omega_k \left(a_k^\dagger a_k + \frac{1}{2} \right) + \frac{g}{n! N^{n/2-1}} \\ \times \sum_{\{k_i\}} v(k_1, \ldots, k_n) \Delta(k_1 + \cdots + k_n) A_{k_1}, \ldots, A_{k_n}, \end{aligned} \tag{4}$$

$$\begin{aligned} \gamma_k &= 1 - e^{ik}, \quad v(k_1, \ldots, k_n) = \prod_{l=1}^{n} \frac{\gamma_{k_l}}{\sqrt{\omega_{k_l}}}, \\ g &= \frac{g_0}{\hbar\omega_0} \left(\frac{\hbar}{2m\omega_0} \right)^{n/2}, \quad A_k = a_k + a_{-k}^\dagger. \end{aligned} \tag{5}$$

Further $\Delta(k)$ is unity when $k = 2\pi j$, where j is an integer or else it is zero.

III. PHONON RELAXATION RATE

As mentioned above the noninteger power dependence q^δ of relaxation rate $\Gamma(q)$ for the $n = 4$ potential arises due to a scattering process already seen at the second order. This corresponds to the diagram given in Fig. 1(a) with three internal lines joining the two interaction vertices. For this diagram the collision integral diverges as $q \to 0$ and leads to the relaxation rate of the form $\Gamma(q \to 0) \sim q^{5/3}$ for small q [13]. The other contributions like vertex corrections were found to yield analytical corrections, which did not change the leading-order wave-vector dependence of $\Gamma(q)$. This leads us to first examine the second-order self-energy diagrams for the higher-order potentials as well.

For even potentials with $n = 6, 8, \ldots$, the second-order diagrams that contribute to the relaxation rate can have two kinds of lines. The first kind are those that join the two interaction vertices to be termed as v lines. The second kind are those that form loops on each vertex. Note that there must be the same number m of loops on the two vertices. These are shown in Figs. 1(b) and 1(c). What matters for our discussion is the number r of the v lines in the diagram, as the loops simply contribute to renormalization of the coupling

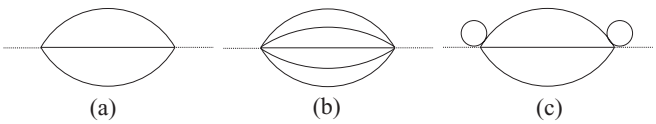

FIG. 1. Second-order self-energy diagrams. Lines represent unperturbed Green's functions D_0. (a) Second-order diagram for $n = 4$. The other two diagrams are for $n = 6$: (b) with five v lines and (c) with three v lines and one phonon loop on each vertex.

of a lower-order potential. To illustrate the point consider the sixth-order potential. There are two kinds of diagrams, one with five v lines [Fig. 1(b)] and one with three v lines and a loop at each vertex [Fig. 1(c)]. Clearly Fig. 1(c) is like the self-energy of the fourth-order potential with renormalized coupling. Thus the number of v lines is the decisive factor for determining the analytic behavior of the diagram. For the nth order potential the number of v lines, $r = n - 1 - 2m$, varies from $n-1$ to 3 in diagrams that contribute to the relaxation rate.

For any even $n \geqslant 4$, we have one diagram of the type in Fig. 1(c) with $r = 3$ which is qualitatively equivalent to the $n = 4$ case. We will now argue that the contributions from diagrams with $r > 3$ are all analytic and lead to $\Gamma(q \to 0) \sim q^2$.

The self-energy contribution for a diagram with r v lines and m loops on each vertex is given by

$$\Sigma^{(2)}(q,\tau) = \frac{g_m^2}{r!N^{r-1}} \sum_{k_1,\ldots,k_r} |v(-q,k_1,\ldots,k_r)|^2 \times \Delta(-q+k_1+\cdots+k_r) \prod_{l=1}^{r} D_0(k_l,\tau), \quad (6)$$

where g_m denotes the renormalized coupling and $D_0(k_l,\tau)$ the free phonon Green's function given by

$$D_0(k,\tau) = \sum_{s=\pm} n_s(k) e^{s\omega_k \tau}, \quad (7)$$

where $n_-(\omega) = (e^{\beta\omega}-1)^{-1}$ and $n_+(\omega) = 1 + n_-(\omega)$, and β is the inverse temperature. The relaxation rate is obtained as $\Gamma(q) = -\mathrm{Im}\Sigma(q, iw_n \to \omega_q + i0^+)$, where $\Sigma(q,i\omega_n) = \int_0^\beta d\tau e^{i\omega_n\tau}\Sigma(q,\tau)$. Here $\omega_n = 2n\pi/\beta$ are the Matsubara frequencies. Choosing the Brillouin zone $[0,2\pi)$ and using wave-vector conservation, we get

$$\Gamma_r(q) = \frac{\pi g_m^2}{r!}\omega_q(1-e^{-\beta\omega_q}) \sum_{\{s_l\}} \prod_{l=1}^{r-1} \int_0^{2\pi} \frac{dk_l}{2\pi}\, \omega_{k_l} n_{s_l}(\omega_{k_l}) \times \omega_{k_r} n_{s_r}(\omega_{k_r}) \delta\left(\omega_q - s_r\omega_{k_r} - s_{r-1}\omega_{k_{r-1}} - R\right), \quad (8)$$

where $R = \sum_{l=1}^{r-2} s_l \omega(k_l)$ and

$$k_r = s_r\left(2j\pi - P + q - s_{r-1}k_{r-1}\right), \quad (9)$$

with $P = \sum_{l=1}^{r-2} s_l k_l$. The integer $j \equiv j(\{s_l\},\{k_l\},q)$ is chosen so that k_r lies within $[0,2\pi)$. The process corresponding to $j = 0$ is normal while $j \neq 0$ corresponds to umklapp. The prefactor $\omega_q(1-e^{-\beta\omega_q})$ makes $\Gamma_r(q)$ proportional to $\omega^2(q)$ for small q, provided the integral on the right-hand side of Eq. (8) is finite at $q = 0$. We shall now show that this is so for $r > 3$. To see this, note that factors of $n(\omega_k)\omega_k$ in the integrand do not affect the singular behavior of the integral at $q = 0$, as they are rather smooth as a function of their variables. To analyze the singular behavior of the integral, we may replace them by constants. The energy δ-function leaves us with an integral over $r-2$ variables which we choose to be $k_1,\ldots,k_{r-2}$. The δ- function defines a surface $S \equiv (k_1,\ldots,k_{r-2})$ by

$$f \equiv \omega(q) - s_{r-1}\omega(k_{r-1}) - s_r\omega(k_r) - R = 0, \quad (10)$$

where k_r is given by Eq. (9). We now define the collision integral $I(q)$ as follows

$$\Gamma_r(q \to 0) \sim \omega^2(q) I(q), \qquad I(q) = \sum_{\{s_l\}} \int_S d\boldsymbol{k} \frac{1}{|J(q,k_1,\ldots,k_{r-2},\{s_l\})|}, \quad (11)$$

where $d\boldsymbol{k} = dk_1,\ldots,dk_{r-2}$ and the Jacobian $J = (\partial/\partial k_{r-1})f$ is given by

$$J = 2\left\{\sin^2\left(\frac{2j\pi - P + q}{4}\right) - \frac{1}{4}\left[\frac{R}{2} - \sin\left(\frac{q}{2}\right)\right]^2\right\}^{\frac{1}{2}}. \quad (12)$$

The contributions from all the solutions k_{r-1} of Eq. (10) are to be included. The quantity whose square root is taken is guaranteed to be non-negative in S by Eq. (10). Note that J depends on $\{s_l,k_l\}$ through R and P and the integer j as defined in Eq. (9). We need to identify the values of j corresponding to each $\boldsymbol{k}$-space point, but we note that the form of J depends only on whether j is even or odd: the first term within the brackets is $\sin^2[(q-P)/4]$ if j is even, otherwise it is $\cos^2[(q-P)/4]$. Hence we analyze zeros of these two different forms of J; if all those singularities are integrable then $I(q)$ would also be finite.

We now examine if the $(r-2)$-dimensional integrals in Eq. (11) are finite at $q = 0$ for all possible sets of values for $\{s_l\}$. The singularities of the integral come from the zeros of J. We expect the zeros to lie on an $(r-3)$-dimensional subspace S_{sing} in general. Suppose the gradient of J^2, denoted by ∇J^2, is nonzero at a point $\mathbf{k}^* \in S_{\mathrm{sing}}$. A Taylor expansion around $\mathbf{k}^*$ yields $J^2 = \nabla J^2 \cdot (\mathbf{k} - \mathbf{k}^*) +$ higher order terms. Then we choose a local coordinate system in the following way. Define one of the coordinates to be along the normal to S_{sing} at $\mathbf{k}^*$ as $p_1(\mathbf{k}^*) = \nabla J^2 \cdot (\mathbf{k} - \mathbf{k}^*)$. The other coordinates $p_2(\mathbf{k}^*),\ldots,p_{r-2}(\mathbf{k}^*)$ are chosen to form a local coordinate system in S_{sing} at $\mathbf{k}^*$. Then, up to lowest order, $J \sim \sqrt{p_1(\mathbf{k}^*)}$, around this point. The contribution to the integral from a small neighborhood around $\mathbf{k}^*$ may be estimated as

$$I_{\mathbf{k}^*} \propto \int dp_1(\mathbf{k}^*) \frac{1}{\sqrt{p_1(\mathbf{k}^*)}}, \quad (13)$$

which is finite. Now consider points in S_{sing} where ∇J^2 is zero. In general, these points form an $(r-4)$-dimensional subspace of S_{sing} as the additional condition $\nabla J^2 = 0$ has to be satisfied. For this subspace, the procedure described above no longer works and we need to explicitly study the nature of the singularity there. We consider $r = 3$ and $r = 5$ cases explicitly in the following.

For $r = 3$, we have $J_{q=0} = 2\cos^2(k_1/4)$ for all $\{s_l\}$ and S_{sing} is just the point $k_1 = 2\pi$. The gradient of J^2 is zero at this point and we have $J(2\pi - k_1) \sim k_1^2$. This singularity is nonintegrable and we have to study the behavior of the integral in Eq. (11) for finite q as $q \to 0$. This is done in Ref. [13] to obtain $I(q \to 0) \sim q^{-1/3}$.

We next consider a special case of $r = 5$. Choose $s_1 = s_2 = s_3 = 1$ and $s_4 = s_5 = -1$, which correspond to two phonons from the bath scattering the external phonon to produce three

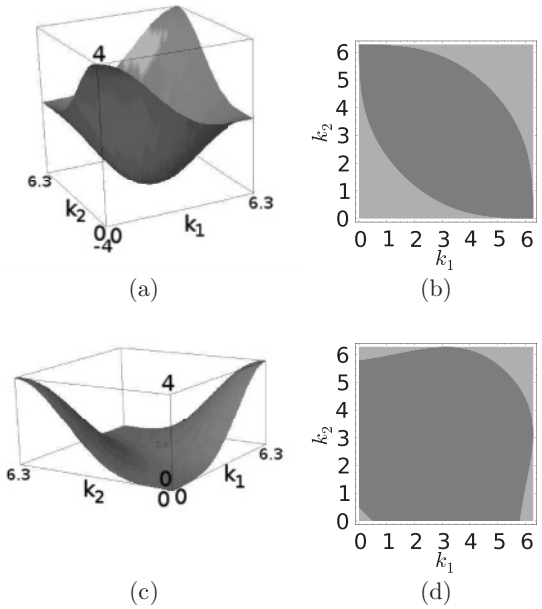

FIG. 2. Plots of $J^2(k_1,k_2,k_3)$ and its zero-value contours. (a) $J^2(k_1,k_2,0)$, (b) zero-value contour of $J^2(k_1,k_2,0)$, (c) $J^2(k_1,k_2,2\pi)$, and (d) zero-value contour of $J^2(k_1,k_2,\pi)$. In the contour plots, only the light-colored region can be part of S whereas J^2 is negative in the darker region.

phonons. For odd j, the Jacobian is obtained as

$$J = 2\left\{\cos^2\left(\frac{k_1+k_2+k_3-q}{4}\right) - \frac{1}{4}\left[\sin\left(\frac{k_1}{2}\right) + \sin\left(\frac{k_2}{2}\right) + \sin\left(\frac{k_3}{2}\right) - \sin\left(\frac{q}{2}\right)\right]^2\right\}^{\frac{1}{2}}. \quad (14)$$

Here S_{sing} is a two-dimensional subspace of S. To see this, we plot $J^2(k_1,k_2,0)$ in Fig. 2(a) and its zero-value contour in Fig. 2(b). This contour is the subset of S_{sing} at $k_3 = 0$ and it separates the $(k_1,k_2,0)$ space into two regions: only the light-colored region that lies outside the contour can be part of S whereas within the darker region, enclosed by the contour, $J^2 < 0$. In Fig. 2(a) it can be seen that the J^2 surface will cut a zero-value surface at an angle, i.e., with nonzero gradient, except at points $(0,2\pi,0)$ and $(2\pi,0,0)$. These two points belong to the one-dimensional subspace where ∇J^2 is zero.

Let us consider the point $(0,2\pi,0)$. In variables $(k_1,k_2 = 2\pi - q_2,k_3)$, we have $J^2 \approx -q_2(k_1+k_3)$, up to the lowest order. This region does not belong to S since $J^2 < 0$ there. But the neighborhood $B_\delta = \{(0,2\pi - q_2,0), q_2 < \delta\}$, with δ being infinitesimal and positive, belongs to S with $J \approx q_2^2/8$ making the q_2 integration divergent. However, the three-dimensional volume measure associated with this neighborhood is zero. (Contrast this with the divergent integral $\int dx x^{-2}$ where the neighborhood of the singular point $x = 0$ has nonzero measure.) In this situation, we take the contribution to the integral in a limiting sense: consider a sequence of integrals $I_{\mathbf{k},n}$, for positive integers n, defined as the contribution to $I(q)$ from $B_{\delta,n} = B_\delta \backslash B_{\frac{\delta}{n}}$ and take $\lim_{n\to\infty} I_{\mathbf{k},n}$. Since $B_{\delta,n}$ does not contain the point $q_2 = 0$, we have finite $1/J$ here and $I_{\mathbf{k},n} = 0$ since the volume measure is zero. Therefore $\lim_{n\to\infty} I_{\mathbf{k},n} = 0$ as well. Similar analysis gives a finite contribution from the point $(2\pi,0,0)$ as well.

At other values of k_3, the shape of the zero-value contour changes, but we can perform similar analysis to find finite contribution to the integral. For example, Fig. 2(c) shows plots of J^2 at $k_3 = 2\pi$ and Fig. 2(d) the zero-value contour-plot of J^2 at $k_3 = \pi$. Note that for $k_3 = 2\pi$, the points where ∇J^2 is zero form the line $(k_1,k_1,2\pi)$ around which $J^2(k_1,k_1,2\pi - q_3) \approx -2\sin(k_1/2)(\cos(k_1/2)+1)q_3$, upto leading order, is negative unless $q_3 = 0$. But in the neighborhood $\{(k_1+q_1,k_1+q_2,2\pi), |q_i| < \delta\}$, having zero three-dimensional volume, we have $J^2 \approx (q_1-q_2)^2/4$ being positive. Again we estimate the contribution to $I(q)$ to be finite, following the limiting procedure discussed earlier.

Now, we try to see some generic features with the help of the contour plots in Fig. 2. One feature we notice for these cases is that the subspace in which $\nabla J^2 = 0$ lies on the boundary of the cube $[0,2\pi] \times [0,2\pi] \times [0,2\pi]$. For example, note the points $(0,2\pi,0),(2\pi,0,0),(k_1,k_1,2\pi)$, etc. The integration space S only contains the region that lies outside the contour, the light-colored region in the contour plots. But at the boundary an infinitesimal neighborhood in S around the singular points has a volume measure equal to zero and hence the contribution to the integral is zero as discussed earlier. We have checked this for a finite set of values of k_3, but our guess is that the feature is true for all values of k_3.

The analysis of J for even j follows a similar path. For example J^2 for $k_3 = 2\pi$ is exactly the same as the odd j case with $k_3 = 0$. And we find a finite contribution from this also. So, the contribution to $I(q)$ is finite for this particular set of $\{s_i\}$. We expect the contribution from other $\{s_i\}$, many of which allow for zero or very small volumes of integration (regions where $J^2 > 0$), also to be finite, thus concluding that the contribution from the $r = 5$ diagrams is proportional to q^2. Continuing the analysis for higher r values this way is impractical. However, with increased dimensionality of the integrals, we find it highly unlikely that diagrams with $r > 5$ will show singular behavior. From these considerations we surmise that only the diagram with three v lines has a singular behavior, which gives the leading-order phonon relaxation rate $\Gamma(q \to 0) \sim q^{5/3}$. Further support for this analysis is provided by numerical computations on thermal conductivity for chains with polynomial potentials with powers $n = 4$, 6, and 8, which we present in the next section.

IV. NUMERICAL COMPUTATIONS

We have performed a numerical study of the system using a classical molecular dynamics simulation. The Hamiltonian is given by Eq. (1) and the potential is taken to be of the form given by Eq. (2). The system was attached to Nosé-Hoover thermostats at the two ends [16,17]. This procedure introduces two thermostat variables, ζ_1 and ζ_N, and the dynamical equations get modified as

$$\begin{aligned}
\frac{d}{dt}x_i &= p_i/m, \\
\frac{d}{dt}p_i &= F(x_i - x_{i-1}) - F(x_{i+1} - x_i) - \delta_{i,1}\zeta_1 p_1 - \delta_{i,N}\zeta_N p_N, \\
\frac{d}{dt}\zeta_1 &= \frac{p_1^2}{2T_1} - 1, \quad \frac{d}{dt}\zeta_N = \frac{p_N^2}{2T_N} - 1, \qquad (15)
\end{aligned}$$

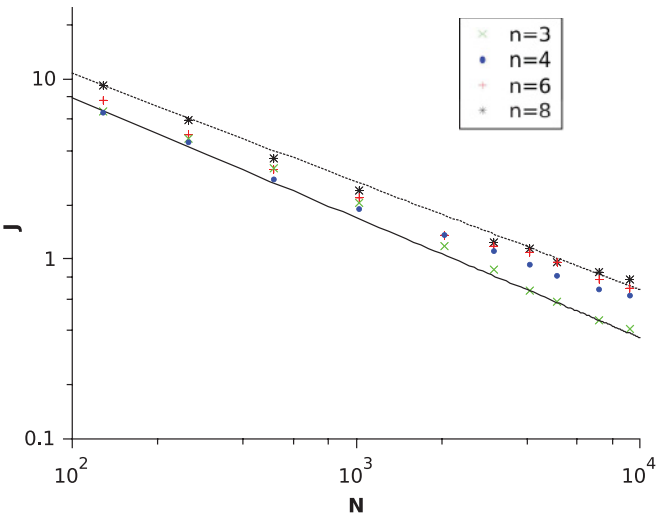

FIG. 3. (Color online) Dependence of the current density J on the system size N for different nonlinearities, n, of the pair potential. We have drawn two lines as an aid to the eye for comparison of the data: the dotted and solid lines have slopes (in the log-log scale) $-3/5$ and $-2/3$, corresponding to $\alpha = 2/5$ and $\alpha = 1/3$, respectively.

where $F(x) = -(d/dx)V(x)$ and T_1 and T_N are the temperatures at ends 1 and N, respectively. The expression for local heat flux can be obtained in the following way. Write the Hamiltonian $H = \sum_i h_i$, where the local energy is given by

$$h_i = \frac{p_i^2}{2m} + \frac{1}{2}\left[V(x_i - x_{i-1}) + V(x_{i+1} - x_i)\right]. \qquad (16)$$

Then, the choice

$$j_i = [h_i, h_{i-1}]_{\rm PB} = \frac{1}{2m}\left(p_i + p_{i-1}\right) F(x_i - x_{i-1}) \qquad (17)$$

satisfies the energy continuity equation $dh_i/dt = j_i - j_{i+1}$. Here $[.,.]_{\rm PB}$ stands for Poisson bracket.

We define j to be the average of j_i over all sites except boundaries and the thermal conductivity can be estimated using the formula

$$\kappa(N) = jN/(T_1 - T_N). \qquad (18)$$

For the simulation we choose $m = \omega_0 = 1$, $T_1 = 152$, and $T_N = 100$. Also we take $g_0 = (n-1)!/10$ such that the nonlinear part of $F(x)$ becomes $-0.1\,x^{n-1}$. Equations (15) are integrated using an adaptive-step-size-controlled method that uses Runge-Kutta Pince-Dormand integration scheme, provided by the GNU Scientific Library [18]. After neglecting a transient time of 200 000, we calculate the average of j_i over time 500 000. The results for $n = 3$, 4, 6, and 8 are reported in Fig. 3 for N up to 9216. For the case of $n = 3$, we add a stabilizing term, $x^4/400$, to the potential $V(x)$. To analyze the dependence of N, we plot j as a function of N and see that $j \sim N^{\alpha-1}$. Thus we estimate $\alpha \approx 2/5$ for $n = 4$, 6, and 8 and $\alpha \approx 1/3$ for $n = 3$.

V. CONCLUSION

To conclude, we have presented an analysis to show that the relaxation rate $\Gamma(q)$ of phonons at small wave-vectors q for even polynomial interaction potentials has the form $\Gamma(q) \propto q^{5/3}$. The basis for this conclusion lies in the circumstance that this fractional exponent arises due to just one scattering process for which the scattering integral diverges as $q \to 0$. Though the detailed calculations are for potentials for powers $n = 4$ and $n = 6$, arguments based on diagrammatic analysis provide strong evidence that this behavior is generic to all even-power potentials. Our theoretical analysis is bolstered by numerical computations for thermal conductance for even potentials of powers $n = 4$, 6, and 8. All these potentials show exponents nearly equal to 2/5 for the divergence of the conductivity. In an earlier paper, we had found a similar situation for cubic and higher odd interactions [14]. For these, $\Gamma(q) \propto q^{3/2}$ for small q. We also report here numerical results for the conductivity of a chain with cubic potential with the addition of a stabilizing quartic potential. Here we find a distinct value close to 1/3 for the exponent. This allows us to argue that there are two universality classes for thermal conduction of vibrational chains which just depend on whether the interaction potential is even or not. In a sense these results match the hydrodynamic analysis of Lee-Dadswell *et al.* [8] and the mode-coupling analysis of Delfini *et al.* [10], but with a difference. The two α exponents in the above two calculations are 1/2 and 1/3, whereas we find them to be 2/5 (even) and 1/3 (odd). For this reason it is interesting to contrast our approach with those mentioned above. In our approach the key input is the dispersion of the modes and the momentum-energy conservation in the collision integral. So the difference can possibly be due to the umklapp nature of the singular scattering process and the nonlinear dispersion of modes. The hydrodynamic and classical mode-coupling approaches ignore the lattice effects by taking the dispersion of modes to be linear and not accounting for the umklapp process.

ACKNOWLEDGMENT

We are very grateful to Ashwani Tripathi for help with the numerical computations.

[1] S. Lepri, R. Livi, and A. Politi, Phys. Rep. **377**, 1 (2003).
[2] F. Bonetto, J. L. Lebowitz, and L. Rey-Ballet, in *Mathematical Physics* (World Scientific, London, 2000), p. 128.
[3] S. Lepri, R. Livi, and A. Politi, Europhys. Lett. **43**, 271 (1998).
[4] T. Hatano, Phys. Rev. E **59**, R1 (1999).
[5] P. Grassberger, W. Nadler, and L. Yang, Phys. Rev. Lett. **89**, 180601 (2002).
[6] T. Mai, A. Dhar, and O. Narayan, Phys. Rev. Lett. **98**, 184301 (2007).
[7] O. Narayan and S. Ramaswamy, Phys. Rev. Lett. **89**, 200601 (2002).

[8] G. R. Lee-Dadswell, B. G. Nickel, and C. G. Gray, Phys. Rev. E **72**, 031202 (2005).
[9] S. Lepri, Phys. Rev. E **58**, 7165 (1998).
[10] L. Delfini, S. Lepri, R. Livi, and A. Politi, Phys. Rev. E **73**, 060201(R) (2006).
[11] A. Pereverzev, Phys. Rev. E **68**, 056124 (2003).
[12] J. Lukkarinen and H. Spohn, Comm. Pure Appl. Math. **61**, 1753 (2008).
[13] Santhosh G. and D. Kumar, Phys. Rev. E **76**, 021105 (2007).
[14] Santhosh G. and D. Kumar, Phys. Rev. E **77**, 011113 (2008).
[15] Santhosh G. and D. Kumar, Phys. Rev. E **82**, 011130 (2010).
[16] S. Nosé, J. Chem. Phys. **81**, 511 (1984).
[17] W. G. Hoover, Phys. Rev. A **31**, 1695 (1985).
[18] Reference manual for GNU Scientific Library, http://www.gnu.org/software/gsl/manual/html_node/Ordinary-Differential-Equations.html.